Geochemistry, Geophysics, Geosystems

METHOD
10.1029/2025GC012621

Key Points:

- New generation shipboard gravimeters implemented on research vessels in the U.S. Academic Research Fleet with better operational capabilities
- Performance evaluation of the new gravimeter in varied sea-states demonstrates high stability under different operation modes
- Gravity data acquisition and quality assessment workflow are summarized with recommendations for best practices for users to follow

Supporting Information:

Supporting Information may be found in the online version of this article.

Correspondence to:
J.-N. Wu,
jyun-nai.wu@whoi.edu

Citation:
Wu, J.-N., Tominaga, M., Mark, H., Zhu, J., Fornari, D., Tivey, M., et al. (2026). Shipboard marine gravimeters operated on vessels in the U.S. Academic Research Fleet: Capabilities and data quality. *Geochemistry, Geophysics, Geosystems*, *27*, e2025GC012621. https://doi.org/10.1029/2025GC012621

Received 18 SEP 2025
Accepted 15 APR 2026

Author Contributions:
Conceptualization: Jyun-Nai Wu, Masako Tominaga
Data curation: Jyun-Nai Wu, Eric Hayden, Marissa Small
Formal analysis: Jyun-Nai Wu
Funding acquisition: Masako Tominaga, Daniel Fornari, Maurice Tivey
Investigation: Jyun-Nai Wu, Thomas Lanagan, Steve Faluotico
Methodology: Jyun-Nai Wu, Hannah Mark

Shipboard Marine Gravimeters Operated on Vessels in the U.S. Academic Research Fleet: Capabilities and Data Quality

Jyun-Nai Wu[1], Masako Tominaga[1], Hannah Mark[1,2], Jian Zhu[1], Daniel Fornari[1], Maurice Tivey[1], Thomas Lanagan[3], Steve Faluotico[3], Eric Hayden[3], Marissa Small[3], Daniel Aliod[4], Nigel Brady[4], Alicia Metzger[5], and Potential Field Pool Equipment program[1]

[1]Department of Geology and Geophysics, Woods Hole Oceanographic Institution, Woods Hole, MA, USA, [2]Marine and Polar Geophysics, Lamont-Doherty Earth Observatory of Columbia University, Palisades, NY, USA, [3]Department of Applied Physics and Ocean Engineering, Woods Hole Oceanographic Institution, Woods Hole, MA, USA, [4]Dynamic Gravity Systems, Broomfield, CO, USA, [5]Office of Geomatic, National Geospatial-Intelligence Agency, St Louis, MO, USA

Abstract Shipboard gravity anomaly data provide high-resolution information for a wide range of Earth and ocean science research as well as ground-truthing US national geodetic modeling. Motivated by the end of life-cycle for legacy Bell aerospace marine Gravity Meter system (BGM-3) gravimeters onboard vessels in the U.S. Academic Research Fleet, a new generation of marine gravimeters from Dynamic Gravity Systems (DGS) was introduced as replacements. We describe the technical functions of this new generation of marine gravimeter and describe an open-source post-processing software package with a simple workflow that users can adapt for processing and assessing data quality along with recommendations on the basis of ~5 years of operational experience with the DGS meter. We demonstrate the capability of the DGS marine gravimeter using data from expeditions conducted on the R/V *Atlantis* and RVIB *N. B. Palmer* that experienced various sea state and operation modes, including open-water, dynamic positioning, and ice-breaking conditions. DGS data collected during both cruises are internally consistent using crossover error analysis. Comparisons between the DGS meter and satellite-derived gravity anomalies imply a constant offset. While shorter-wavelength anomalies imply finer scale seabed features were well resolved, high frequency ship motions show that swell in the open ocean remains the main artifact contributor to marine gravity data that requires filtering. Quality assessments during different operational modes suggest that data recorded by DGS gravimeters are comparable to BGM-3 data, with superior operational characteristics that facilitate a wide range of vessel and research requirements, and better logistical capabilities for global operations.

Plain Language Summary Gravity anomaly data from the world's ocean basins provide fundamental information on mass distributions within the oceanic crust, including seafloor features comprising magmatic, volcanic, and tectonic structures, sedimentary formations, and seabed mineral deposits. Marine gravity data are essential to estimate Earth's geoid, a mathematical description of sea level surface of the Earth. This report introduces a new generation of marine gravimeters recently installed in several U.S. Academic Research Fleet vessels as a part of their permanent shipboard systems for underway geophysical data collection. We analyze gravity data and assess data quality from two expeditions, each of which conducted surveys under different sea state and ocean environments (equatorial open ocean vs. polar region with sea ice). This report concludes with recommendations for the use of these marine gravimeters for academic research when operated in various sea conditions and operational modes.

1. Overview: New Marine Gravimeters on U.S. Academic Research Fleet

Marine gravity anomaly data have applications in Earth, ocean, and planetary science topics and provide insight into Earth's planetary morphology, isostatic compensation, subsurface architecture, and the processes that drive plate geometry and tectonics (e.g., Sandwell & McAdoo, 1988; Sośnica et al., 2015; Watts et al., 2020; Wessel & Watts, 1988; Zhu et al., 2023). Global gravity anomaly estimates from satellite altimetry data have been derived from several missions, including NASA's Gravity Recovery and Climate Experiment (GRACE) and the European Space Agency's Gravity Field and Steady-State Ocean Circulation Explorer (GOCE) (e.g., W. H. F. Smith & Sandwell, 1997). These estimates are further augmented with the higher track density data acquired by the CryoSat-2, Jason-1, and Surface Water and Ocean Topography (SWOT) missions (e.g., Sandwell et al., 2014; Yu

Project administration: Masako Tominaga
Resources: Masako Tominaga, Daniel Aliod, Nigel Brady, Alicia Metzger
Software: Jyun-Nai Wu, Hannah Mark, Jian Zhu
Supervision: Masako Tominaga
Validation: Jyun-Nai Wu
Visualization: Jyun-Nai Wu
Writing – original draft: Jyun-Nai Wu, Masako Tominaga, Nigel Brady
Writing – review & editing: Jyun-Nai Wu, Masako Tominaga, Hannah Mark, Daniel Fornari, Maurice Tivey

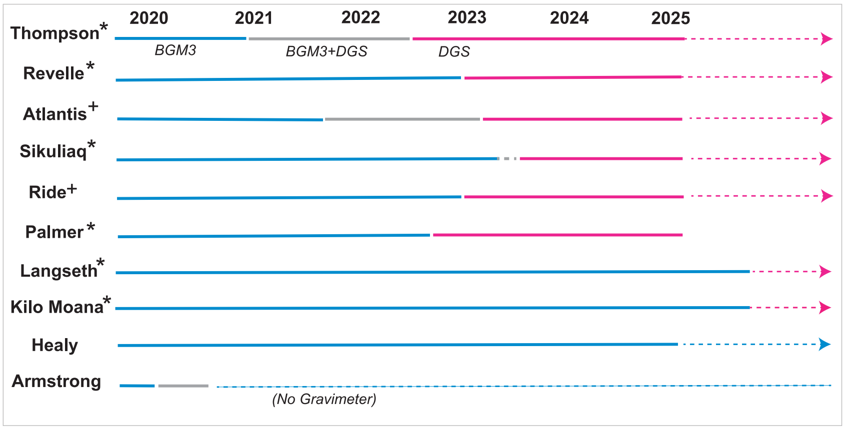

Figure 1. Transition chronology from BGM-3 to DGS gravimeters in the U.S. Academic Research Fleet during the period 2020 to 2025. Blue indicates the duration of BGM-3 gravimeter operations; pink indicates the duration of DGS gravimeter operations; and gray indicates when BGM-3 and DGS gravimeters were operating simultaneously on research cruises. * and + denote gravimeters funded by the National Science Foundation and National Geospatial-Intelligence Agency, respectively.

et al., 2024). Derived gravity data from these satellite measurements include uncertainties which have traditionally been calibrated by comparing them to high-quality data collected by shipboard instruments. Shipboard gravity data collected by the U.S. Academic Research Fleet (ARF) over the past ~60 years have played an important role in "ground-truthing" satellite gravity measurements.

Data collected in the oceans by shipboard gravity sensors on vessels in the University National Oceanographic Laboratory System (UNOLS) ARF continue to be the foundation of the highest precision gravity data at shorter wavelengths compared to satellite. These data are routinely archived by the Rolling Deck to Repository facility (R2R, https://www.rvdata.us/; Carbotte et al., 2022) (Figure 1). Properly acquired and reduced marine gravity data, including land and gravity ties to correct sensor drift over time, are an asset for research and national strategic needs. Underway gravity data also contribute to the missions undertaken by the National Geospatial-Intelligence Agency (NGA), including modeling to derive a more accurate terrestrial geoid, an equipotential surface of Earth's gravity field approximating mean sea level, which serves as a reference for physical heights (Pekeris, 1935; Richards & Hager, 1984; Small & Sandwell, 1992). The geoid is used for strategic calculations by multiple U.S. defense agencies to fulfill their missions.

The concept of a National Science Foundation (NSF)-funded marine gravimeter equipment pool was introduced circa 2004, and the Potential Field Pool Equipment (PFPE) facility at Woods Hole Oceanographic Institution (WHOI) was established in 2009 to serve UNOLS ARF technical support groups in that capacity. PFPE has assisted in operating a pool of BGM-3 marine gravimeters (Bell aerospace marine Gravity Meter system) on many ARF vessels. Until 2020, 7 BGM-3s operated on the R/Vs *Marcus Langseth*, *Kilo Moana*, *Sikuliaq*, *Thomas G. Thompson*, *Sally Ride*, *Roger Revelle*, and *Atlantis* as "permanent" installations (i.e., as part of the ship's routine geophysical data acquisition systems). One other BGM-3 meter operated on an as-needed basis on R/V *Armstrong*, and two BGM-3s were dedicated to operations and data collection on the RVIB *N.B. Palmer* and USCGC *Healy* for polar studies. *Sikuliaq* and *Healy* BGM-3 operations were conducted in collaboration with gravimetry experts at the Geophysical Institute at Univ. Alaska, Fairbanks (e.g., Coakley et al., 2019).

In recent years, the BGM-3 gravimeter systems used in the US ARF have become increasingly difficult to maintain and operate. While these gravimeters produce excellent data, the meters are 30–40 years old, and their bespoke electronics present major challenges for vessel operators' shipboard technical support groups as well as the PFPE supporting gravimeter operations. These challenges include, but not limited to: (a) the meter components are unique, and most of the parts needed to repair and maintain the meters are out of stock/production; (b) the sensor and sensor electronics require continuous power to maintain the calibrated reference mass, hence the meters can never be off power including during shipping and transport; and (c) several components of the BGM-3 are ITAR (International Traffic in Arms Regulations) classified, which limits the ability of users and operators to ship a BGM-3 meter to foreign ports and operate it, or have a vessel containing a BGM-3 to transit through foreign

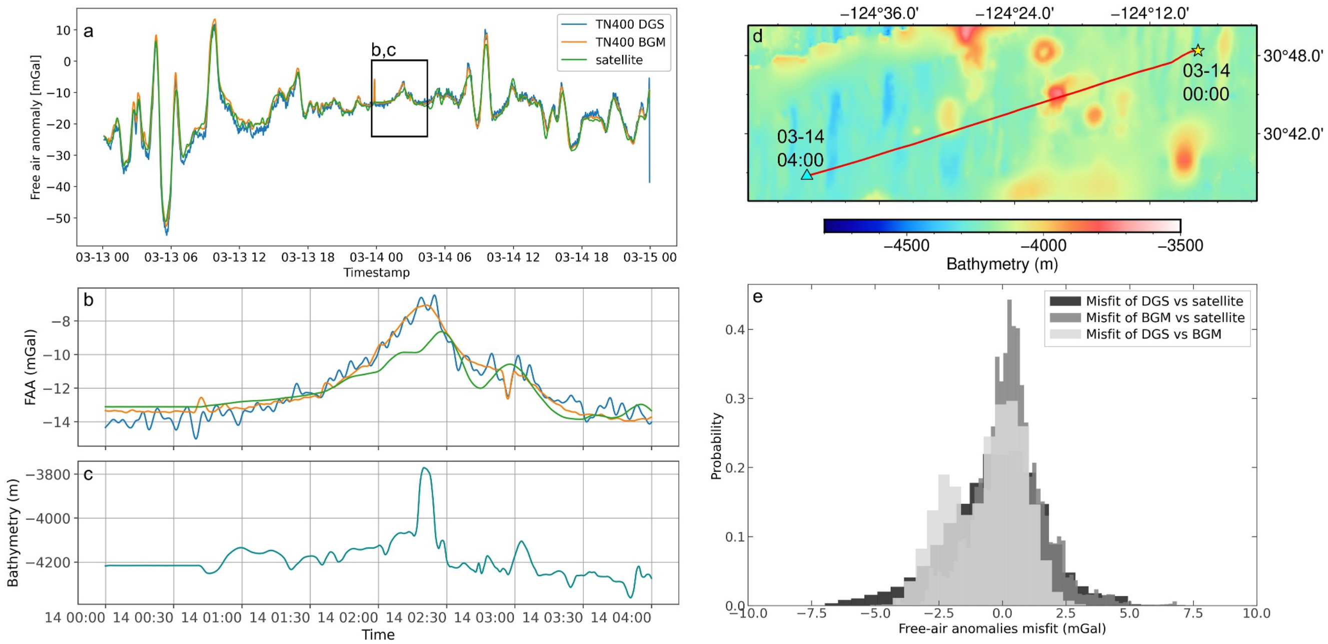

Figure 2. Free-air anomalies estimated from DGS (blue), BGM-3 (orange), and satellite (green) measurements during cruise TN400. The overall long-wavelength trends agree one to the other among these three and short-wavelength trends agree between the DGS and BGM3 measurements. (a) Overall free-air anomalies time series. Black box indicates panels (b and c) for zoom-in plot. (b) Zoom-in free-air anomalies time series across a topographic high. (c) Corresponding bathymetry along the track from GEBCO (2025). (d) Bathymetric map overlayed with tracks in panels (b and c). (e) Histogram of misfit between DGS, BGM, and satellite, showing that the data quality between DGS and BGM is compatible (equivalent RMS level).

territorial waters. The effort of sourcing and/or salvaging parts for BGM-3s has been a resource consuming process, and the limited availability of parts poses increasing challenges to maintaining stable daily operations. Especially taxing vessel operators and shipboard technicians' resources is the nature of the BGM-3's electrical components. BGM-3 meter contain electromechanical sensors that require extensive maintenance and care in handling/shipping. This has become a major challenge when ships enter a yard period during which power may be intermittently interrupted on short notice. These situations have required complex logistics and arrangements to ensure that the BGM-3 sensor was on stable power and monitored routinely. The ITAR status and regulations surrounding BGM-3 use and shipping have also been difficult to manage.

To overcome the technical and operational challenges associated with vintage BGM-3 gravimeters, PFPE began replacing BGM-3 gravimeters in the ARF with Dynamic Gravity Systems (DGS) gravimeters in 2020 (Figure 1). Initial performance verification was completed during two expeditions in 2020–2021, where PFPE collected data from BGM-3 and DGS meters simultaneously and demonstrated that DGS gravimeter results agreed well with BGM-3 data, as well as longer-wavelength satellite-derived free-air gravity anomalies (Tominaga et al., 2021; Figure 2). DGS AT1M systems have now been installed on R/Vs *Sikuliaq*, *Thompson*, *Sally Ride*, *Roger Revelle*, *Atlantis*, RVIB *Palmer*, and R/V *Marcus G. Langseth* (Figure 1). In the sections that follow, we describe DGS gravimeter operation principles in comparison with its predecessor BGM-3 and assess examples of DGS gravimeter data from both open-ocean and polar-ocean cases. We also present recommendations for the marine geophysical user community based on the mechanical principles and data quality of the DGS gravimeter.

2. Data and Methods

2.1. DGS Gravimeter Principle

The operational principle of the DGS gravimeter is the suspension of a "gravitational sensing mass" by a very stable metal spring with low temperature-sensitivity (Torge, 1989). Small variations in local gravity are measured based on the current in an electromagnetic (Lorentz force) actuator, combined with a position detector to keep the sensing spring at a constant length and the mass in the "null" position (e.g., Gupta, 2012; Tinto et al., 2019; Yamakawa & Yamazaki, 2014). The DGS sensor is a scalar gravity force sensor mounted in a 2-axis gyroscope, which keeps the sensitive axis of the gravimeter aligned with local gravity, with the meter recording the magnitude of the vector.

The DGS gravimeter consists of three important components:

1. A spring balance sensor, which has a small test mass mounted at one end of a horizontal beam and a frictionless hinge at the other end, is balanced by a specially designed metal spring which has a zero unstressed length (the zero-length spring) and effectively has infinite displacement sensitivity so it can detect changes in gravity of better than 1 part in 10^7 or 0.1 milli-gals.
2. The spring is kept at its unstressed length by a force feedback system and a beam position detector. Changes in gravity are measured by the amount of force required to keep the beam at its zero-displacement position and the spring at a constant unstressed length.
3. The sensor maintains alignment with the local vertical gravity in a two-axis (pitch and roll) gimbal controlled by accelerometers, to determine the local vertical gravity over a period of 4 min, with gyroscopes controlling torque motors to counteract the motion of the ship. The results of this study indicate that the system can continuously collect gravity data in sea conditions up to the WMO (World Meteorological Organization) sea state 5 (2.5–4 m wave height). The appropriate threshold for clamping the system still needs to be evaluated in future tests.

The gravimeter has a worldwide range to measure gravity anomalies without range scale adjustment. In addition to minimizing the effect of dynamic accelerations on the ship from wave motion, the sensor is designed to be insensitive to ambient temperature changes between 5°C and 40°C. The sensor is also insensitive to pressure changes due to weather conditions and magnetic field variations. The metal spring is heat treated so that it has a very low drift-rate (~3 mGal/month in the initially, decreasing to 0.5 mGal/month after a few years of operation) and the gimbal is designed to minimize the transmission of vibrations into the sensor, which would increase the noise level inherent in the gravity data (DGS; https://www.dynamicgravitysystems.com).

2.2. DGS Data Format and Metadata

DGS gravimeters typically acquire data at 1 Hz and are time-synced with the ship's Global Positioning Satellite (GPS) feed (latitude, longitude, time). Four monitors record cross-coupling factors used to correct gravity responses from horizontal accelerations (Jacoby & Schulze, 1967). The DGS system outputs data strings from a serial feed to the ship's system in two ways: raw and processed (file extensions can depend on how each vessel's data pipeline to R2R is handled; for example, there are files with .raw and .proc extension). The raw files contain "counts" values recorded by the meter, which can be used to calculate the gravity signal with a set of calibration constants. Exact format descriptions for the raw data string can be found at the manufacturer's site in the AT1M manual (https://www.dynamicgravitysystems.com/tools). The processed files contain the gravity values calculated from those raw measurements but are not processed further to remove bias or calculate gravity anomalies.

Users will almost always want to work with the processed data files for further analysis, and those files are the primary data archived at R2R. Gravimeter data and related vessel attitude, position and speed data can typically be downloaded from R2R after an embargo period following a given research cruise (Carbotte et al., 2022). The processed data files are also saved locally during a cruise on the DGS QA laptop in files with names that start with "AT1M." The exact data format in the processed files varies between UNOLS vessels, and the PFPE-developed python package *shipgrav* can ingest vessel-specific data strings (Mark, Zhu, Tominaga, Tivey, & Aliod, 2024). The current code is tuned for each vessel's data format as of Q1 2025, and will be updated in the future if vessel-specific data formats change.

Importantly, while the DGS gravimeter is configured to ingest navigation data from the ship's feed and includes these coordinates in the gravity output files, the synchronization can be lost and the navigation data in the gravity files is not always reliable. The best way to ensure accurate navigation data is to match timestamps between the gravimeter files and separate navigation feeds from the ship's GPS.

2.3. Example DGS Data From AT50-31 and NBP2501 Expeditions

To assess the instrument response to various operational conditions, we used DGS gravimeter data acquired during AT50-31 on R/V *Atlantis* and NBP25-01 on RVIB *N. B. Palmer*. During the AT50-31 expedition (11 November–17 December 2024), DGS AT1M-21 marine gravimeter data were integrated with GNSS (Global

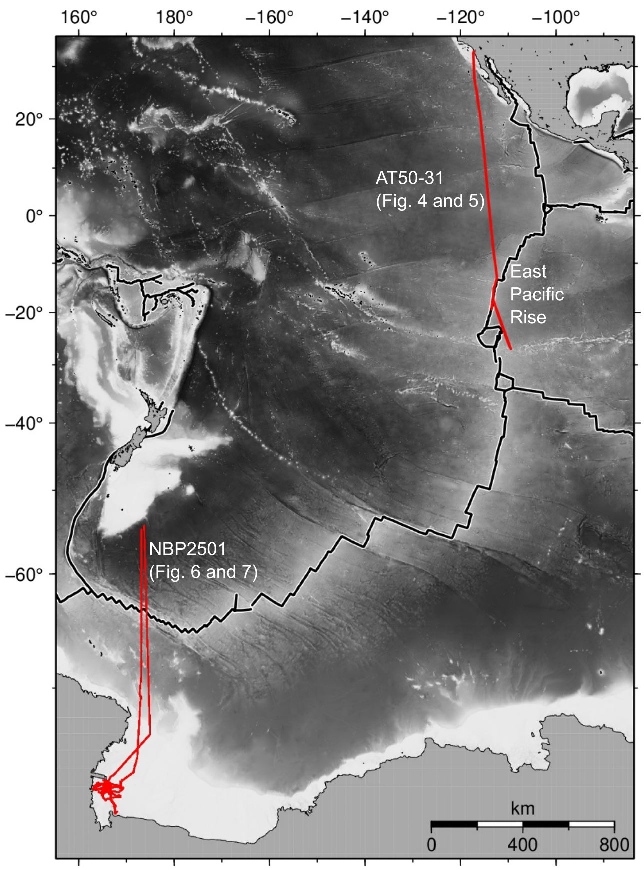

Figure 3. Locations of the AT50-31 and NBP2501 cruises' track lines (red lines) along which DGS marine gravimeter data were obtained and used in this study. The underlying map is GEBCO 2024 (GEBCO Compilation Group, 2024).

Navigation Satellite System) navigation from the ship's Seapath 385 (NMEA $…GGA string) with a numeric position resolution of ~0.02 m. AT50-31 started in San Diego, CA and ended at Easter Island (Figure 3). Gravity ties were carried out before and after the cruise with a Lacoste-Romberg land meter ("G"-meter) at known absolute gravity stations located within the Scripps Institution of Oceanography's Marine Facility in San Diego, Pt. Loma, CA. Bias between the DGS gravimeter and absolute gravity measurements was determined by comparing values between the dock site and the known site (e.g., Ince et al., 2020; Watts et al., 2020; Wessel & Watts, 1988). The biases measured at the beginning and end of the cruise increased ~0.5 mGal, showing that the DGS gravimeter drifted slightly during the cruise. It should be noted that the sensor was kept on during the transit through the Exclusive Economic Zone (EEZ) of Mexico and Chile (Easter Island) but data collection was prohibited, hence the data gaps (Figure 4). This cruise had two main modes of operation: a transit in the open ocean, and holding-station to support deep submergence vehicle operations. We present gravity data analytics for each of these modes (Figures 5a and 5b, respectively).

During the NBP2501 on RVIB *Palmer* (14 February–7 April 2025), DGS AT1M-27 marine gravimeter data were integrated with Seapath 330 and 380 GNSS navigation positions with a resolution ~0.02 m. The NBP2501 expedition started from Lyttelton, New Zealand, traveled to the Ross Sea, Antarctica and then returned to Lyttelton (Figure 3). Land ties were carried out before and after the cruise with the same protocol as the AT50-31 cruise noted above, and the biases were determined by comparing values between the dock site and the absolute gravity station located within the Magnetic Observatory of the Botanic Garden in Christchurch, New Zealand. The measured biases increased ~1 mGal from beginning to end (i.e., ~0.5 mGal/month drift rate). Data collection began once the ship left the EEZ of New Zealand and ended when the ship re-entered the EEZ (Figure 6). Operational modes for this cruise included transits in open water, ice breaking, and transiting in sea ice-dampened, no-wave conditions. Gravity data analytics for these modes are shown in Figures 6–8 and Figures S1–S3 in Supporting Information S1.

2.4. Data Quality Assessment With Free Air Gravity Anomalies

Free Air Anomalies (FAA) were calculated via a typical post-processing workflow using gravimeter data from cruises AT50-31 and NBP2501 (Mark, Zhu, Tominaga, Tivey, & Aliod, 2024). We first calibrated the DGS gravity measurements with gravity tie measurements to absolute level. We further reduced the gravity by subtracting the theoretical gravity on the GRS80 ellipsoid (Hinze et al., 2005). We applied a solid earth tide correction to remove the time-varying gravitational effects (Longman, 1959). Lastly, we applied an Eötvös correction for the vertical component of the Coriolis and centrifugal accelerations resulting from ship's motion (Harlan, 1968).

We first demonstrate the data quality comparison between the DGS and BGM systems using data from R/V *Thompson*, which carried both systems onboard during a transit cruise TN400 (Figure 2). The overall trend of FAA estimates from DGS and BGM both agree with the satellite FAA, while the DGS FAA shows more high-frequency signal than the BGM (Figure 2b). Histograms of misfit between the DGS, BGM, and satellite data demonstrate that both systems provide equivalent data quality (Figure 2e).

We evaluated the internal consistency of the FAA by assessing the crossover error (COE; e.g., Wessel & Watts, 1988). Crossover points are defined as points occurring spatially within a 5-m radius (equal to the distance traveled in 1 s at a maximum travel speed of 10 knots, i.e., ~5 m/s), which ensures we detect at least one point with 1 Hz sampling rate. COE during the AT50-31 cruise is 0.09 ± 5.5 mGal (Figure 5e), which is similar to previous studies (e.g., Wessel, 1989, 2010). Further, we calculated the misfit between free-air anomalies from the DGS gravimeter and independently derived FAA from satellites (Yu et al., 2024). The misfit is 9.7 ± 6.5 mGal, which

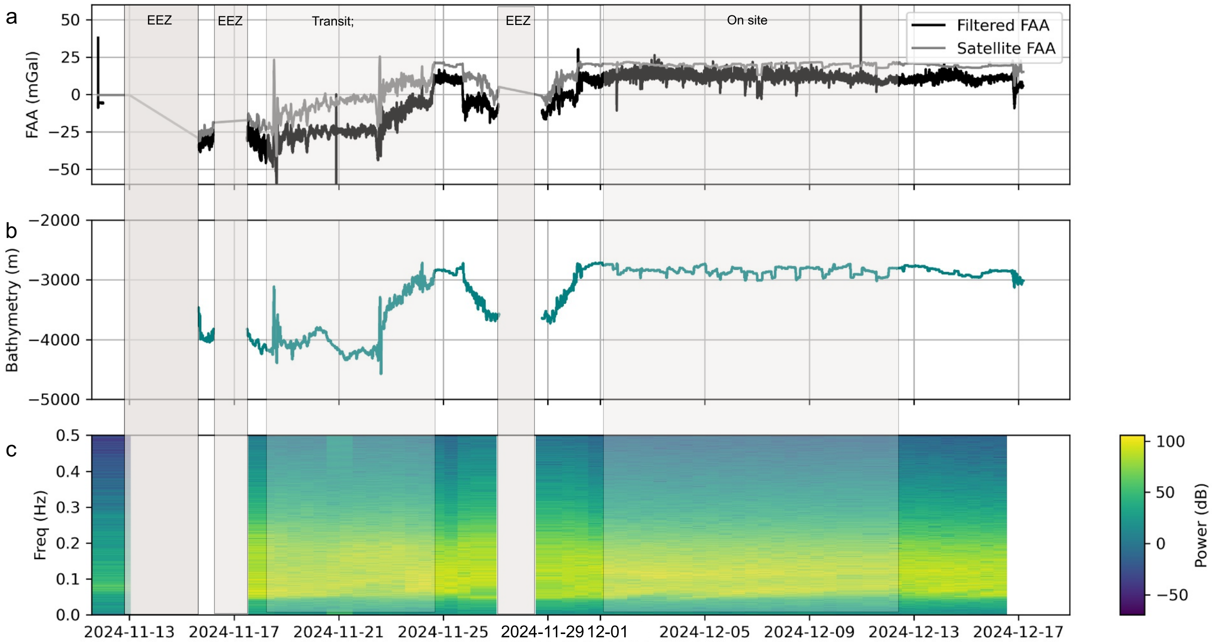

Figure 4. Overview of data acquired by AT1M-21, a DGS marine gravimeter, during the entire duration of AT50-31 (37 days). (a) The free-air anomalies (FAA) calculated from the DGS gravimeter (black line) and satellite (gray line), (b) corresponding underway bathymetry, and (c) spectrogram of raw FAA. Gray zones mark the time period of EEZs and different operation mode periods.

is similar to previous comparisons (e.g., 6.5–8.2 mGal; Neumann & Forsyth, 1993; Small & Sandwell, 1992) with overall trends in agreement with each other. For NBP2501, the COE is 0.01 ± 1.5 mGal and the misfit between the DGS and satellite-derived FAA is −2.6 ± 2.8 mGal. The misfits may imply constant offsets between the DGS meter and satellite data, which may be due to imperfect bias estimation or short-wavelength signals that are missing in satellite-derived data downward continuation.

3. Expedition-Based Marine Gravity Data Assessment

3.1. Effects of Modes of At-Sea Operation on the Quality of Data

DGS marine gravimeters mechanically and electrically compensate for the motion of a moving platform to optimize its measurements of the gravity field. However, this compensation may not be perfect when platform motion exceeds certain thresholds. At sea, vessel motions are caused by a combination of the weather and sea-state conditions and the mode of operation, such as in-transit, holding-station, or ice-breaking. The ability of gravimeters to compensate for platform acceleration has been widely discussed for different types of instruments (Dehlinger, 1978; Jacoby & Schulze, 1967; LaCoste, 1967). Here, we assess DGS instrument performance under different modes of operation and weather conditions. We calculate the signal-to-noise ratio (SNR) (Text S1) and spectrograms of ship roll and pitch to evaluate the relationships between ship motion and gravity measurements (Figures 4c and 6c; Figures S4 and S5 in Supporting Information S1). We estimate the standard deviation of raw gravity with a moving window of 200 s to help assess the data quality (Figure S6 in Supporting Information S1). Note that ship's heading information is taken into account by the Eötvös correction.

The open water transit mode of gravimeter operation during the AT50-31 cruise provides an opportunity to assess how the DGS gravimeter behaves in typical underway conditions (e.g., 10 kts along a consistent heading). **The holding-station mode of gravimeter operation** during the AT50-31 cruise provides gravity field measurements when the platform is exposed to higher-frequency three-dimensional motions while the Dynamic Positioning system operates within a mixed swell (Figure 4). The AT50-31 cruise transited from ~20°N to 17°S and arrived at the southern East Pacific Rise on 2024-11-21 where the FAA started increasing due to mid-ocean ridge topography (Figure 4). Once on-site, the ship stayed mostly around the mid-ocean ridge axis of the southern East Pacific Rise and the FAA remained higher than what was recorded during the transit mode (Figure 4).

10.1029/2025GC012621

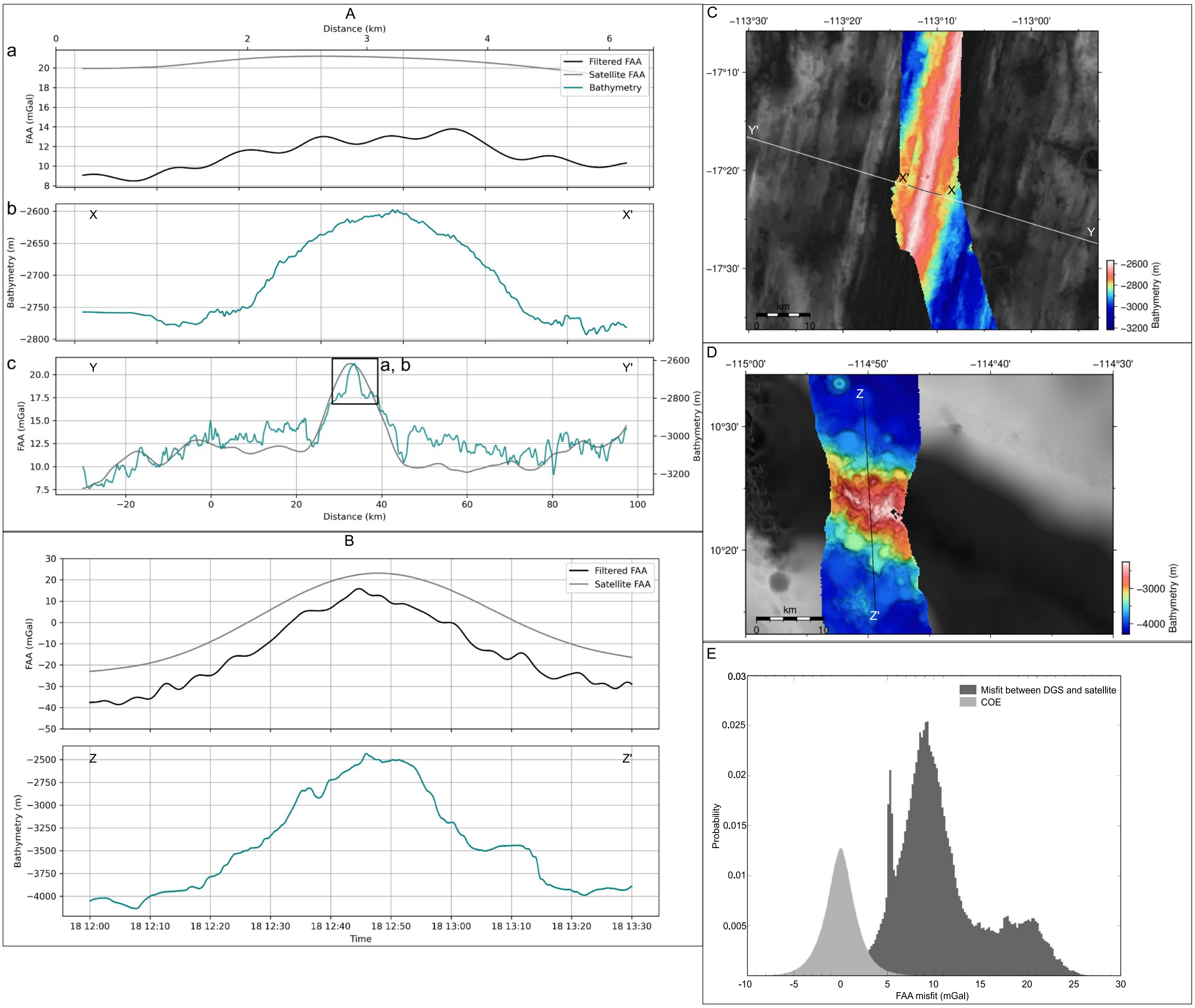

Figure 5. (a) Free-air anomalies calculated from DGS gravimeter (black line) and satellite (gray line) and (b) corresponding shipboard bathymetry (100 m resolution) and (c) extended profile across fast-spreading mid-ocean ridge crest during on-site (panel A) and transit period (panel B). Maps showing ship track during on-site (panel C) and during transit (panel D). Histograms of crossover error and misfit between filtered free-air anomalies calculated from DGS and from satellite during AT50-31 (panel E).

We applied a 200 s low-pass filtering over free-air gravity anomalies during on-site and transit modes. The resulting SNR are −29 and −32 dB for the transit and on-site periods, respectively (Figure 5). SNR was only slightly lower during the on-site period compared to the transit. The comparison of DGS and satellite derived free-air anomalies shows that the DGS data contain higher frequency signals that are compatible with shipboard multibeam bathymetry collected during AT50-31 (Figure 5).

The ice-breaking and icy-sea transit modes of gravimeter operation during the NBP25-01 cruise provide an opportunity to assess how the instrument responds in both breaking sea ice and transit within channels created within the packed ice by the ice breaking. We categorize the mode of operation into transit (Figure S1 in Supporting Information S1), on-site with open water (Figure S2 in Supporting Information S1), and in ice with constant ice breaking (Figure S3 in Supporting Information S1). It should be noted that the mode of icebreaking was mainly by ship's hull pushing and breaking through the packed sea ice, but not the ride-up-and-crush mode. The NBP2501 cruise had relatively little on-site time, and the mean traveling speeds were 10, 3, and 2 knots for transit, on-site, and in ice, respectively. We applied a low-pass filter of 200 s and estimated SNRs of −26, −21,

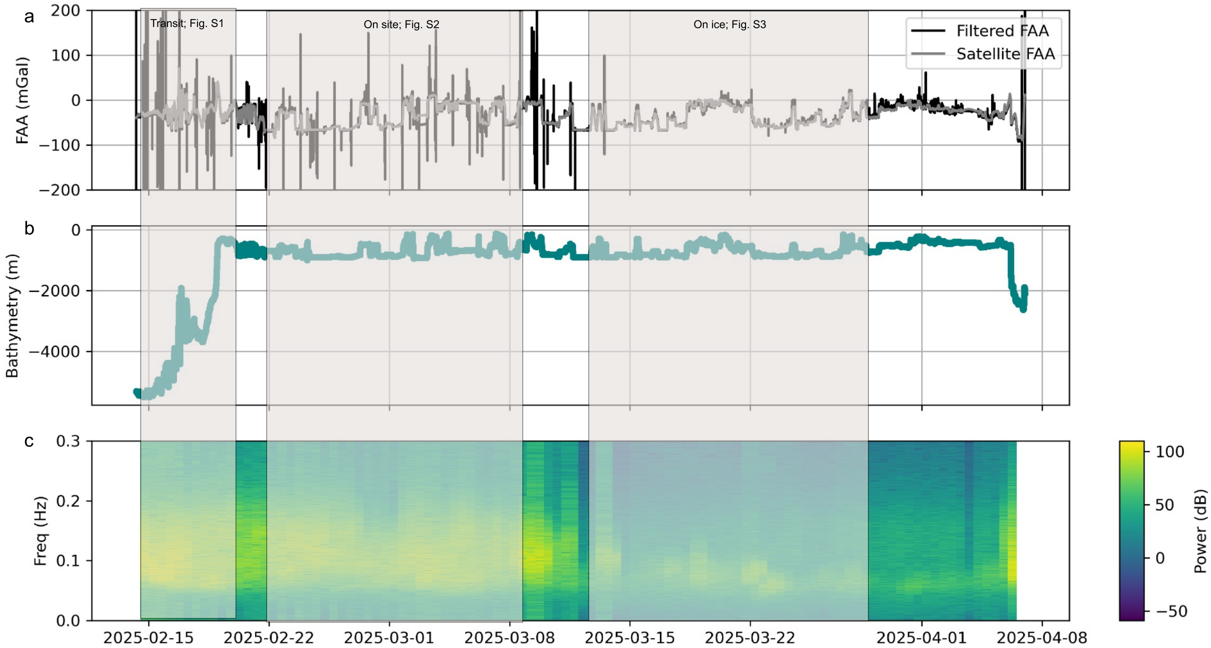

Figure 6. Overview of data acquired during NBP2501. (a) The free-air anomalies (FAA) calculated from DGS gravimeter (black line) and satellite (gray line), (b) corresponding underway bathymetry (Tominaga et al., 2025), and (c) spectrogram of raw FAA. Gray zones mark the time period when traveling through EEZs and different operation modes period. Spikes in panel (a) were due to the sea state of the southern ocean and/or rapid turning.

and −10 dB for transit, on-site, and in ice. SNR is highest during the ice phase, and is similar during transit and on-site periods. One example from a mapping survey of repeated lines of breaking ice and mapping back along the broken route shows a slightly better SNR in the repeated path and both paths show overall agreement to shipboard bathymetry (Figure 7; Tominaga et al., 2025).

In open water, for both AT50-31 and NBP2501, the unfiltered FAA has the most power at frequencies of 0.1–0.15 Hz, which corresponds to 6–10 s period. This frequency band agrees with swell frequency (e.g., Lucas & Guedes Soares, 2015). The strongest signal is from ship roll, which has a generally higher amplitude in the frequency domain than ship pitch (Figure S4 in Supporting Information S1). The unfiltered FAA spectrogram during the transit phase of AT50-31 has a wider-band of high amplitude, whereas two clearer high-power bands at 0.1 and 0.15 Hz occurred during the on-site phase (Figure S4 in Supporting Information S1). The two clear high-power bands may be consistent with the model of a mature swell (Lucas & Guedes Soares, 2015) that consists of older (lower frequency) and fresh waves (higher frequency), and both appear to impact the gravity measurements. We therefore suggest that the ship motions are mostly dominated by swell (reflected in roll and pitch; Figure S4 in Supporting Information S1), and the gravimeter is strongly affected by this motion during on-site periods by a mature swell signal.

During the NBP2501 cruise, the spectrogram amplitudes of free-air anomalies, ship roll, and pitch all decrease around 2025-03-14 (Figure S4 in Supporting Information S1). The spectral power density of raw gravity, free-air anomalies, ship roll, pitch, and heave shows that the energy in the band of 0.08–0.12 Hz decreases by at least an order of magnitude during in-ice periods (Figure S5 in Supporting Information S1). The energy of raw gravity drops four orders of magnitude during the in-ice period (Figure S6 in Supporting Information S1). The SNR increases from −23 to −13 dB after 2025-03-14. We speculate that the main contribution of noise is from swell, which dies down after the sea ice is compacted (Figure 8). Sea ice status evolves from "open drift" to "close packs" to "compact" (O. Smith, 2007). During the open drift phase, sea ice drifts freely in pancake shapes (Figure 8a). These pancakes further evolve into a close pack (Figure 8b), and eventually the sea will be completely covered by compact ice (Figure 8c). When sea ice completely covers the sea surface, it may dampen the swell propagation from the far field. Meanwhile, the ice breaking motion mostly involves ship's hull pushing and breaking through the packed sea ice, which makes the ship vibration less intense. Furthermore, due to ice breaking motion, the ship travels at a lower speed, which is optimal for gravity surveying. Although intuitively the ice-

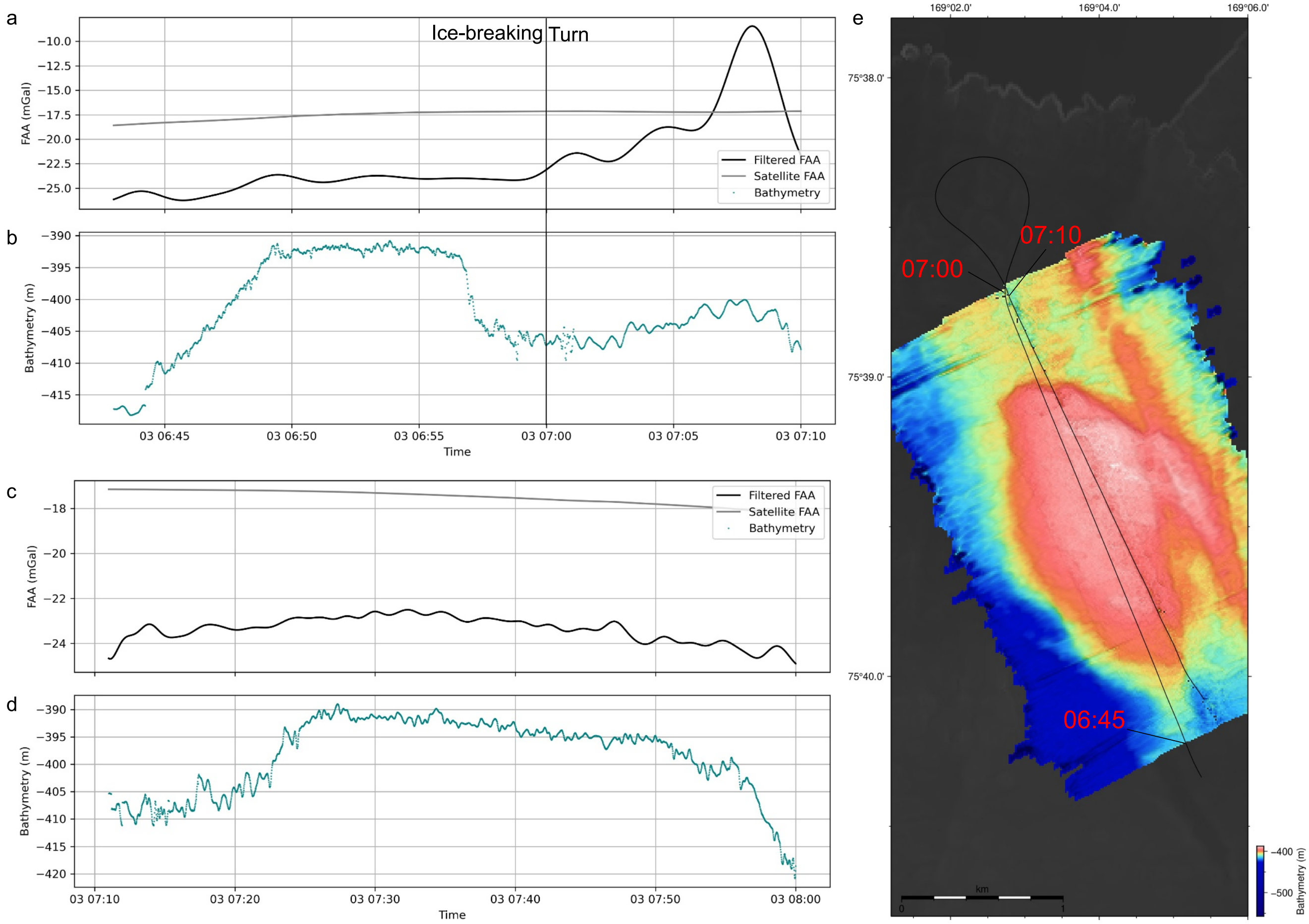

Figure 7. Example of mapping survey during ice breaking period. The ship began breaking ice at 2025-04-03 06:40 (UTC) and turned around to retrace the same route at 07:10, mapping along the broken ice route. Panels on the left show free-air anomalies and bathymetry during ice breaking (a and b) and retracing (c and d). (e) Map on the right shows the trackline of ship and shipboard bathymetry (Tominaga et al., 2025).

breaking motions may degenerate the gravity data quality, the performance of the DGS meter is better during the ice-breaking phase than during transit or on-site phases.

3.2. Cross-Coupling Corrections for the DGS AT1M Meters

In principle, ship accelerations and the observed gravity corrected for the Eötvos effect should be uncorrelated, but in practice, the signal measured by a shipboard gravimeter is affected by the motion of the ship (LaCoste, 1967). We therefore correct for some of the kinematic effects of ship motion using a cross-coupling correction. The DGS AT1M uses a design that is theoretically susceptible to cross-coupling effects, unlike the legacy BGM-3 meters. Cross-coupling corrections are made by describing the ship's acceleration in terms of several independent monitors, measuring the correlation between monitors and the observed gravity, and adding a weighted linear combination of the monitors to the gravity signal to reduce the correlation (Schwarz & Li, 1997; Sun et al., 2007; Valliant, 1991). The four monitors output by the DGS system are (a) ***ve***, square of the beam velocity; (b) ***vcc***, longitudinal accelerometer output multiplied by beam position, calibrated by circular motion in a vertical plane; (c) ***al***, longitudinal accelerometer output multiplied by beam position, calibrated by diagonal motion up and down a ramp; and (d) ***ac***, cross accelerometer output multiplied by beam velocity.

Tests using data from DGS instruments on ARF vessels have shown that the magnitude of the cross-coupling correction is typically small compared to the gravity signal. For the two operational modes (on-site and transit) discussed in this report during AT50-31, the cross-coupling coefficients were negligible (Figures S7 and

10.1029/2025GC012621

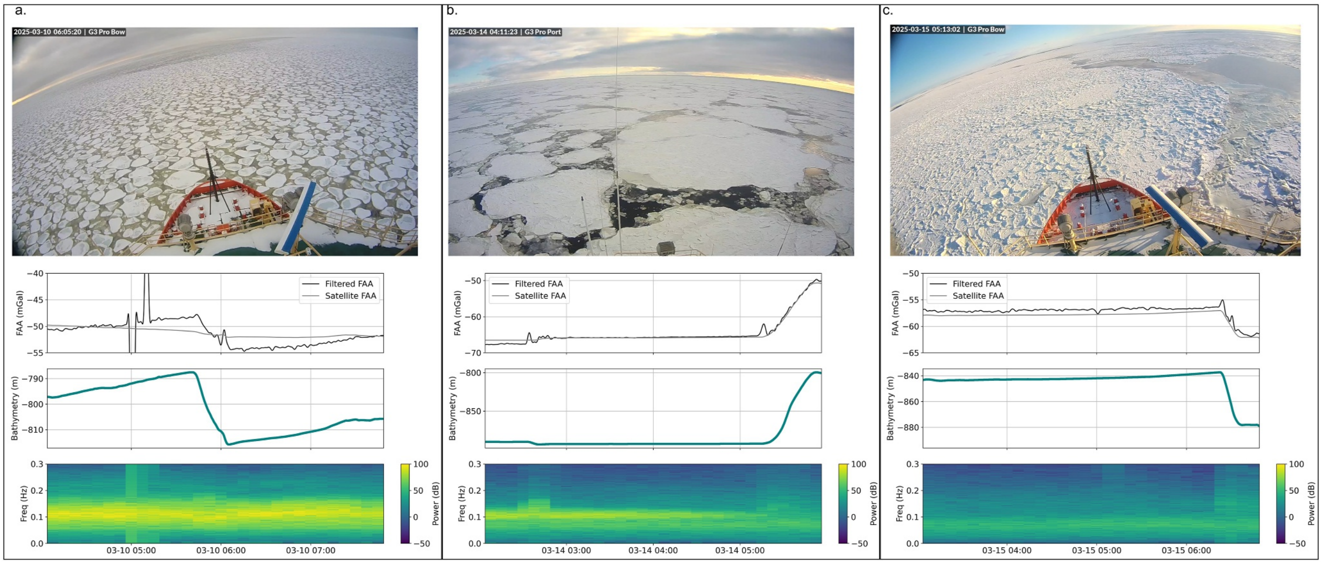

Figure 8. Transition of sea ice evolution between 2025-03-10 and 2025-03-15 and the corresponding gravity record and spectrogram during underway. For each panel, sea images on top and free-air gravity data, bathymetry, and spectrogram of free-air gravity. (a) Open drift ice. (b) Closing packs. (c) Compact ice. SNRs are −24, −18, and −15 dB for a, b, and c periods. The spikes in panel (a) were during quick turns.

S8 in Supporting Information S1). However, the correction may sometimes be important for data collected in rough seas.

Since the cross-coupling correction is calculated by linear regression between the free air anomaly and monitor outputs, the regression coefficients will be most stable and robust if several days of continuous data are used to compute them. Including data collected at different headings with respect to the prevailing wind and waves helps to ensure that the monitors are fully independent in the regression. Cross coupling coefficients for a particular meter installation are not expected to vary significantly over time; hence, values calculated for an installation may be applied to future data sets as long as the meter is not moved.

4. Recommendations

Based on the two examples presented in this report, we recommend that DGS gravimeter users consider the following for operations and data processing: (a) for open sea operations, use data collected while underway instead of during station-holding; (b) in polar regions, data acquired in ice-packed ocean after breaking a channel may be of high quality due to the effects of surrounding ice dampening the swell, and therefore users might consider gravity as an alternative survey when ice-breaking prevents other operations from taking place; (c) gravity bias generally increases ~0.5 mGal per month, so users and shipboard technical groups should be aware of the importance of getting up-to-date gravity tie data (pre- and post-cruise) when processing gravity and compare in-port data to satellite data to get a proper correction; (d) users should pay close attention to filter settings while processing data, which could be potentially affected by swell; (e) users should always calculate cross-coupling coefficients and decide whether to apply them to their processed data by comparing filtered FAA with satellite derived FAA especially for surveys collected in rough seas; and (f) users should take care to properly parse GPS and ship attitude data from their original source instead of from the raw DGS data stream.

The data quality examination demonstrated in this report can serve as a simple workflow example for users to evaluate their own data sets. Users should always seek to conduct a more comprehensive analysis to apply proper corrections for crossover errors and/or ship motions.

Conflict of Interest

The authors declare no conflicts of interest relevant to this study.

Availability Statement

AT50-31 and NBP2501 data are available at R2R (2024, 2025). Software and instructional materials mentioned in this study are available from Mark, Zhu, Tominaga, Aliod, and Tivey (2024).

Acknowledgments

We thank SSSG and crew members of R/V *Atlantis*; and US Antarctic Program ship technicians and crew members of RVIB *N. B. Palmer*. We thank Dr. Bernard Coakley and Dr. Brian Boston for their insightful comments, which improved our work. Figures are generated using Generic Mapping Tools (Wessel et al., 2019) and Python scripts. We thank Daniel Scheirer of USGS-Menlo Park for his contribution to initial at-sea testing and data assessment of DGS gravimeters on R/V *Armstrong*. We also recognize the important contributions of Mr. Randall Herr (now deceased) to the overall improvements in marine gravimetry instrumentation and operations over the past three decades and his collaborations with both WHOI-PFPE and NGA colleagues. This project is funded by the National Science Foundation with award number: National Science Foundation award OCE-1824508, -2015229, -2420887, -2234277, and -2517543 and Office of Naval Research-DURIP award N00014-23-1-2475. The AT1M-21 and -25 are owned by the National Geospatial-Intelligence Agency's gravimeter loan program and loaned to PFPE through the Cooperative Research and Development Agreement. The views expressed in this document do not necessarily reflect those of the National Geospatial-Intelligence Agency, the Department of War, or any other agency of the US Government.

References

Carbotte, S. M., O'Hara, S., Stocks, K., Clark, P. D., Stolp, L., Smith, S. R., et al. (2022). Rolling Deck to Repository: Supporting the marine science community with data management services from academic research expeditions. *Frontiers in Marine Science*, *9*, 1–16. https://doi.org/10.3389/fmars.2022.1012756

Coakley, B., Johnson, J., Beale, J., Ganley, R., & Youngman, M. (2019). Improving the Arctic Gravity Project grid and making a gravity anomaly map for the State of Alaska. *GFF*, *141*(4), 308–315. https://doi.org/10.1080/11035897.2019.1633396

Dehlinger, P. (1978). In P. Dehlinger (Ed.), *Marine gravity*. Elsevier.

GEBCO Compilation Group. (2024). *The GEBCO 2024 Grid*. NERC EDS British Oceanographic Data Centre. https://doi.org/10.5285/1c44ce99-0a0d-5f4f-e063-7086abc0ea0f

GEBCO Compilation Group. (2025). GEBCO 2025 Grid. https://doi.org/10.5285/37c52e96-24ea-67ce-e063-7086abc05f29

Gupta, S. V. (2012). Electronic balances and effect of gravity. In *Mass metrology* (pp. 65–88). Springer.

Harlan, R. B. (1968). Eotvos corrections for airborne gravimetry. *Journal of Geophysical Research*, *73*(14), 4675–4679. https://doi.org/10.1029/jb073i014p04675

Hinze, W. J., Aiken, C., Brozena, J., Coakley, B., Dater, D., Flanagan, G., et al. (2005). New standards for reducing gravity data: The North American gravity database. *Geophysics*, *70*(4), 25–32. https://doi.org/10.1190/1.1988183

Ince, E. S., Förste, C., Barthelmes, F., Pflug, H., Li, M., Kaminskis, J., et al. (2020). Gravity measurements along commercial ferry lines in the Baltic Sea and their use for geodetic purposes. *Marine Geodesy*, *43*(6), 573–602. https://doi.org/10.1080/01490419.2020.1771486

Jacoby, A.-W., & Schulze, R. (1967). New method to eliminate the cross-coupling effect in gravity measurements at sea. *Journal of Geophysical Research*, *72*(8), 2199–2207. https://doi.org/10.1029/jz072i008p02199

LaCoste, L. J. B. (1967). Measurement of gravity at sea and in the air. *Review of Geophysics*, *5*(4), 477–526. https://doi.org/10.1029/rg005i004p00477

Longman, I. M. (1959). Formulas for computing the tidal accelerations due to the Moon and the Sun. *Journal of Geophysical Research*, *64*(12), 2351–2355. https://doi.org/10.1029/jz064i012p02351

Lucas, C., & Guedes Soares, C. (2015). On the modelling of swell spectra. *Ocean Engineering*, *108*, 749–759. https://doi.org/10.1016/j.oceaneng.2015.08.017

Mark, H., Zhu, J., Tominaga, M., Aliod, D., & Tivey, M. (2024). shipgrav: A Python package for marine gravimetry (v1.0.6) [Software]. *Zenodo*. https://doi.org/10.5281/zenodo.14199590

Mark, H. F., Zhu, J., Tominaga, M., Tivey, M., & Aliod, D. (2024). shipgrav: A Python package for marine gravimetry. *Journal of Open Source Software*, *9*(103), 10–12. https://doi.org/10.21105/joss.07358

Neumann, G. A., Forsyth, D. W., & Sandwell, D. (1993). Comparison of marine gravity from shipboard and high-density satellite altimetry along the mid-Atlantic Ridge 30.5°-35.5°S. *Geophysical Research Letters*, *20*(15), 1639–1642. https://doi.org/10.1029/93gl01487

Pekeris, C. L. (1935). Thermal convection in the interior of the Earth. *Geophysical Journal International*, *3*, 343–367. https://doi.org/10.1111/j.1365-246x.1935.tb01742.x

R2R. (2024). AT50-31 cruise [Dataset]. *R2R*. https://doi.org/10.7284/910851

R2R. (2025). NBP2501 cruise [Dataset]. *R2R*. https://doi.org/10.7284/910896

Richards, M. A., & Hager, B. H. (1984). Geoid anomalies in a dynamic Earth. *Journal of Geophysical Research*, *89*(B7), 5987–6002. https://doi.org/10.1029/jb089ib07p05987

Sandwell, D. T., & McAdoo, D. C. (1988). Marine gravity of the Southern Ocean and Antarctic margin from Geosat. *Journal of Geophysical Research*, *93*(B9), 10389–10396. https://doi.org/10.1029/jb093ib09p10389

Sandwell, D. T., Müller, R. D., Smith, W. H. F., Garcia, E., & Francis, R. (2014). New global marine gravity model from CryoSat-2 and Jason-1 reveals buried tectonic structure. *Science*, *346*(6205), 65–67. https://doi.org/10.1126/science.1258213

Schwarz, K., & Li, Z. (1997). An introduction to airborne gravlmet boundary value problems. In F. Sanso & R. Rummel (Eds.), *Geodetic boundary value problems in view of the one centimeter geoid*. Springer. https://doi.org/10.1007/BFb0011709

Small, C., & Sandwell, D. T. (1992). A comparison of satellite and shipboard gravity measurements in the Gulf of Mexico. *Geophysics*, *57*(7), 885–893. https://doi.org/10.1190/1.1443301

Smith, O. (2007). *Observers guide to sea ice* (Vol. 30). Department of Commerce, National Oceanic and Atmospheric Administration, National Ocean Service, Office of Response and Restoration, National Environmental Satellite, Data, and Information Service, National Ice Center.

Smith, W. H. F., & Sandwell, D. T. (1997). Global sea floor topography from satellite altimetry and ship depth soundings. *Science*, *277*(5334), 1956–1962. https://doi.org/10.1126/science.277.5334.1956

Sośnica, K., Jäggi, A., Meyer, U., Thaller, D., Beutler, G., Arnold, D., & Dach, R. (2015). Time variable Earth's gravity field from SLR satellites. *Journal of Geodesy*, *89*(10), 945–960. https://doi.org/10.1007/s00190-015-0825-1

Sun, Z., Xia, Z., & Li, Y. (2007). Cross-coupling correction for LaCoste & Romberg airborne gravimeter. *Geo-Spatial Information Science*, *10*(3), 163–167. https://doi.org/10.1007/s11806-007-0081-5

Tinto, K. J., Padman, L., Siddoway, C. S., Springer, S. R., Fricker, H. A., Das, I., et al. (2019). Ross Ice Shelf response to climate driven by the tectonic imprint on seafloor bathymetry. *Nature Geoscience*, *12*(6), 441–449. https://doi.org/10.1038/s41561-019-0370-2

Tominaga, M., Fornari, D., Zhu, J., Tivey, M., Scheirer, D., Harr, R., et al. (2021). A new generation shipboard marine gravimeter by dynamic gravity systems for the UNOLS Academic Research Fleet. In *AGU fall meeting abstracts* (Vol. 2021, p. G35B-0290).

Tominaga, M., Panter, K., Berthod, C., Tivey, M., Wu, J., Preine, J., et al. (2025). Subglacial explosive volcanism in the Ross Sea of Antarctica Check for updates. *Communications Earth & Environment*, 1–7.

Torge, W. (1989). *Gravimetry*. Walter de Gruyter.

Valliant, H. D. (1991). The LaCoste & Romberg air/sea gravity meter: An overview. In R. A. Geyer & M. Ashwell (Eds.), *Handbook of geophysical exploration at sea*. CRC Press. https://doi.org/10.1201/9781351072618

Watts, A. B., Tozer, B., Harper, H., Boston, B., Shillington, D. J., & Dunn, R. (2020). Evaluation of shipboard and satellite-derived bathymetry and gravity data over seamounts in the northwest Pacific Ocean. *Journal of Geophysical Research: Solid Earth*, *125*(10), 1–18. https://doi.org/10.1029/2020JB020396

Wessel, P. (1989). XOVER: A cross-over error detector for track data. *Computers and Geosciences*, *15*(3), 333–346. https://doi.org/10.1016/0098-3004(89)90044-7

Wessel, P. (2010). Tools for analyzing intersecting tracks: The x2sys package. *Computers and Geosciences*, *36*(3), 348–354. https://doi.org/10.1016/j.cageo.2009.05.009

Wessel, P., Luis, J. F., Uieda, L., Scharroo, R., Wobbe, F., Smith, W. H. F., & Tian, D. (2019). The Generic Mapping Tools version 6. *Geochemistry, Geophysics, Geosystems*, *20*(11), 5556–5564. https://doi.org/10.1029/2019GC008515

Wessel, P., & Watts, A. B. (1988). On the accuracy of marine gravity measurements. *Journal of Geophysical Research*, *93*(B1), 393–413. https://doi.org/10.1029/JB093iB01p00393

Yamakawa, Y., & Yamazaki, T. (2014). Mathematical model of checkweigher with electromagnetic force balance system. *ACTA IMEKO*, *3*(2), 9–13. https://doi.org/10.21014/acta_imeko.v3i2.86

Yu, Y., Sandwell, D. T., & Dibarboure, G. (2024). Abyssal marine tectonics from the SWOT mission. *Science*, *386*(6727), 1251–1256. https://doi.org/10.1126/science.ads4472

Zhu, F., Liu, X., Li, Z., Yuan, J., Guo, J., & Sun, H. (2023). High spatial resolution marine gravity trend determined from multisatellite altimeter data over Bay of Bengal. *Geophysical Journal International*, *235*(3), 2257–2267. https://doi.org/10.1093/gji/ggad368

References From the Supporting Information

Yuan, Y., Wu, Z., Gao, J., & Jiang, Z. (2025). Establishing a marine gravimeter test site in the South China Sea to validate the performance of different marine gravimeters. *Remote Sensing*, *17*(1), 14. https://doi.org/10.3390/rs17010014